

Neutron Diffraction from Photoinduced Gratings in a PMMA Matrix

R. A. Rupp, J. Hehmann, and R. Matull

Fachbereich Physik, Universität Osnabrück, D-4500 Osnabrück, Federal Republic of Germany

K. Ibel

Institut Laue-Langevin, 156X Centre de Tri, F-38042 Grenoble CEDEX, France

(Received 4 October 1989)

Utilizing an optical holographic setup thick refractive index gratings are written in poly(methyl methacrylate) (PMMA). We show experimentally that these gratings diffract not only visible light but also cold neutrons.

PACS numbers: 61.12.Gz, 42.40.-i

Holographic methods are a well established tool for the investigation of photorefractive materials, i.e., materials which change their refractive index upon illumination.¹ Certain photorefractive processes like thermal fixing² or photopolymerization³ involve mass transport. As a consequence, not only the optical but also the neutron refractive index may be changed. We report here, for the first time, on neutron diffraction at thick gratings produced by optical holography.

Our sample was a 1.93-mm-thick plate (approximately 25×25 mm²), consisting of a poly(methyl methacrylate) (PMMA) matrix, residual monomer, and the photoinitiator bis(cyclopentadienyl)-titaniumdichloride. When illuminating the sample with the light interference pattern of two coherent plane waves of optical wavelength $\lambda = 514.5$ nm, a photochemical reaction is started. In the course of the chemical reaction diffusion processes take place which build up a mass-density modulation in conformity with the intensity modulation of the light interference pattern. This mass-density modulation is the origin of the optical and neutron refractive-index grating. By an optical diffraction experiment with $\lambda = 632.8$ nm the grating period Λ has been determined to be 361.7 ± 0.1 nm. The grating-containing area of the sample has an elliptical form with extensions 10×18 mm².

The neutron diffraction experiment was performed at the D11 small-angle scattering instrument of the Institute Laue-Langevin (ILL) at Grenoble, France. For our test experiment two hours of beam time were provided.

Wavelength selection at the instrument D11 is done by setting the rotary speed of a mechanical monochromator drum.⁴ A speed of 1832 rpm, as used in our experiment, yields a wavelength distribution with a full width at half maximum of 0.09 nm. According to Ref. 4 the neutron wavelength at the maximum is theoretically $\lambda_n = 1.025$ and experimentally $\lambda_n = 1.01 \pm 0.01$ nm; according to Ref. 5, $\lambda_n = 1.00$ and 0.98 nm, respectively. The uncertainty is partly due to a slight misalignment of the drum's rotary axis.

The sample was placed in the collimated neutron beam (beam divergence $\approx 0.05^\circ$) behind a cadmium dia-

phragm with a clear aperture of 8×11 mm². The diaphragm ensured that neutrons could pass through only the grating-containing area of the sample. The distance between the detector (64×64 ¹⁰BF₃ gas-containing cells of 100-mm² cross section) and the sample was 35 m.

In order to eliminate the effect of gravity on the diffraction pattern the sample was mounted such that the Bragg peaks were to be expected in the horizontal plane. Therefore, the grating vector \mathbf{K} of the refractive-index grating also has to be in the horizontal plane (x - y plane in Fig. 1). By turning the sample around a vertical axis (z axis in Fig. 1), the inclination angle α between the beam axis and the sample normal was varied between -0.16° and $+0.16^\circ$ in steps of 0.04° . The exposure time was 5 min for each angular setting.

For $\alpha = -0.08^\circ$ and $+0.08^\circ$ sharp neutron diffraction peaks could be observed in the neutron spectrum (Fig. 2). The diffraction spots (as well as the primary beam) extended vertically between $z = 19$ and 25 cm while the horizontal spot width is $\Delta x \approx 3$ cm.

Table I shows the integral counting rate for each angular setting. The integration was performed over the whole peak area for the ± 1 st order, respectively. Counting rates of about 10 to 20 counts in 5 min are due to noise. Hence, in the peak maximum, a signal-to-noise ratio of at least 50:1 was reached. The fact that the diffraction peaks almost vanish when turning the sample by 0.04° demonstrates the strong angular selectivity of a thick grating.

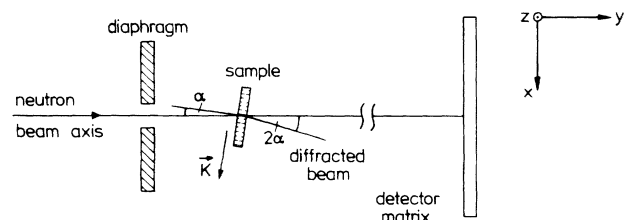


FIG. 1. Schematic drawing of the neutron diffraction setup.

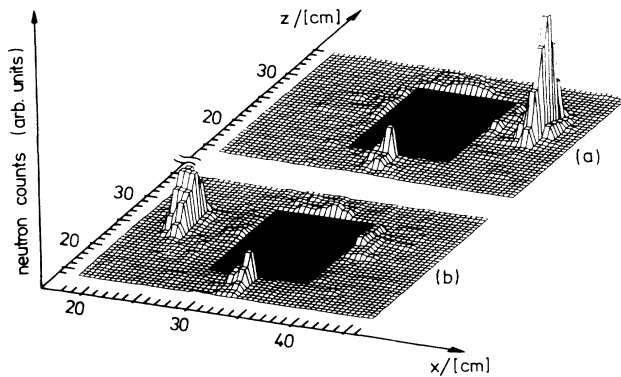


FIG. 2. The neutron counting rate for a section of the detector matrix around the suppressed primary beam in a three-dimensional plot (the black area marks the beam stop). For (a) $\alpha = -0.08^\circ$ the Bragg peak occurs at the right side of the primary beam; for (b) $\alpha = +0.08^\circ$ on the left side. The smaller peak in the middle below the beam stop is due to the slowest neutrons in the velocity spectrum of the primary beam.

With known neutron wavelength one can determine the grating period from the experimental results, or vice versa. As it turns out, the grating period Λ has been measured with high accuracy by optical means; therefore, we prefer to evaluate the corresponding neutron wavelengths.

In principle, there are two possibilities. Using the measured grating period $\Lambda = 361.7$ nm and the Bragg angle $\Theta_B = 0.08^\circ$, one calculates from Bragg's condition $\lambda = 2\Lambda \sin \Theta_B$ a neutron wavelength of $\lambda_n = 1$ nm. Because of the bad angular resolution of the rotary table used in our experiment the Bragg angle Θ_B could not be measured very precisely; therefore, this value for the neutron wavelength only shows an agreement within a large error margin. A second way to calculate the neutron wavelength is to determine the Bragg angle from the distance of the ± 1 st-order Bragg peaks on the detector matrix. Doing this for several z positions within the peak area, a slight increase of the calculated neutron wavelength with decreasing height becomes apparent. This is plausible from ballistic trajectory considerations.⁶ Because of the gravitational forces, slower neutrons reach the detector matrix at lower z positions. On the other hand, the wavelength of slower neutrons is larger and from Bragg's condition it follows immediately that the Bragg angle should increase. The absolute values for the neutron wavelength are in a range that is in agreement with the wavelength distribution expected from Ref. 4.

For a precise quantitative analysis we intend to repeat the neutron diffraction experiment with higher-angular resolution. Then it might be possible to determine not only the maximum neutron wavelength but also the wavelength distribution with high accuracy. This would be interesting for the preparation of an easy-to-handle

TABLE I. Integral counting rate for each angular setting of the sample. The area for the +1st-order peak was from $x = 41$ to 43 cm and from $z = 19$ to 25 cm. For the -1st-order peak x goes from $x = 20$ to 23 cm with the same z values.

Angle α (deg)	+ 1st-order counting rate (counts/5 min)	- 1st-order counting rate (counts/5 min)
-0.16	15	13
-0.12	20	14
-0.08	936	21
-0.04	94	14
0.00	11	17
+0.04	19	13
+0.08	19	677
+0.12	17	32
+0.16	14	9

calibration standard for small-angle neutron diffraction instruments.

Our preliminary experiment demonstrates the feasibility of photoinduced neutron diffraction. Thick-refractive-index gratings produced by optical holography act as neutron refractive-index gratings due to mass-density modulation within the sample. Our rocking curves show a Bragg behavior of the diffracted neutron counting rate which is typical for thick gratings.

Rocking curves with higher-angular resolution and a determination of the diffraction efficiency in order to determine the density modulation are still required and in preparation. Latest experimental results show that the transmission for 1.0-nm neutrons is approximately 20% for a 2-mm-thick sample. The diffraction efficiency is in the range of 0.1%. Higher diffraction efficiencies seem to be predominantly a question of using materials which allow for larger thicknesses.

Neutron diffraction experiments are a new promising tool for the investigation of certain photochemical reactions, for preparing holographic calibration standards for small-angle neutron scattering cameras, and for holographic optical elements for cold and very cold neutrons.

We thank T. Lückmeyer and Dr. H. Franke for assistance in the preparation of PMMA samples and Professor E. Krätzig for his support.

¹P. Günter, Phys. Rep. **93**, 199-299 (1982).

²R. Matull and R. A. Rupp, J. Phys. D **21**, 1556-1565 (1988).

³H. Franke, H. G. Festl, and E. Krätzig, Colloid Polym. Sci. **262**, 213-216 (1984).

⁴K. Ibel, J. Appl. Crystallogr. **9**, 296-309 (1976).

⁵K. Ibel and I. Sosnowska, "Result of an experiment on the OPAL standard," complement to K. Ibel and A. Wright, Institut Laue-Langevin Internal Scientific Report No. 80IB45S, 1988 (unpublished).

⁶K. Ibel, W. Schmatz, and T. Springer, Atomkernenerg./Kerntechnik. **17**, 15-18 (1971).